Oxidation of Nitrided Si(100) by Gaseous Atomic and Molecular Oxygen

Alex L. Gerrard, Jau-Jiun Chen, and Jason F. Weaver*

Department of Chemical Engineering, P.O. Box 116005, University of Florida, Gainesville, Florida 32611

Received: December 7, 2004; In Final Form: February 15, 2005

The nitridation of Si(100) by ammonia and the subsequent oxidation of the nitrided surface by both gaseous atomic and molecular oxygen was investigated under ultrahigh vacuum (UHV) conditions using X-ray photoelectron spectroscopy (XPS). Nitridation of Si(100) by the thermal decomposition of NH_3 results in the formation of a subsurface nitride and a decrease in the concentration of surface dangling bond sites. On the basis of changes in the N1s spectra obtained after NH_3 adsorption and decomposition, we estimate that the nitride resides about four to five layers below the vacuum−solid interface and that the concentration of surface dangling bonds after nitridation is only 59% of its value on Si(100)-(2 × 1). Oxidation of the nitrided surface is found to produce an oxide phase that remains in the outer layers of the solid and interacts only weakly with the underlying nitride for oxygen coverages up to 2.5 ML. Slight changes in the N1s spectra observed after oxidizing at 300 K are suggested to arise primarily from the introduction of strain within the nitride, and by the formation of a small amount of Si_2═N−O species near the nitride−oxide interface. The nitrogen bonding environment changes negligibly after oxidizing at 800 K, which is indicative of greater phase separation at elevated surface temperature. Nitridation is also found to significantly reduce the reactivity of the Si(100) surface toward both atomic and molecular oxygen. A comparison of the oxygen uptake on the clean and nitrided surfaces shows quantitatively that the decrease in dangling bond concentration is responsible for the reduced activity of the nitrided surface toward oxidation, and therefore that dangling bonds are the initial adsorption site for both gaseous oxygen atoms and molecules. Increasing the surface temperature is found to promote the uptake of oxygen when O_2 is used as the oxidant, but brings about only a small enhancement in the uptake of gaseous O-atoms. The different effects of surface temperature on the uptake of O versus O_2 are interpreted in terms of the efficiency at which dangling bond pairs are regenerated on the surface at elevated temperature and the different site requirements for the adsorption of O and O_2.

Introduction

Silicon nitride and oxynitride films have been extensively investigated in recent years due to the advantages afforded by incorporating these materials into the dielectric layers used in metal-oxide-semiconductor (MOS) devices. The addition of small amounts of nitrogen to the SiO_2−Si interface is known to improve the structural quality of the interface and results in lower leakage current across the gate of a MOS device as well as enhanced resistance to boron diffusion into the SiO_2.[1] The low activity of silicon nitride toward oxidation has also proved beneficial to the growth of alternative gate oxides such as Ta_2O_5 and ZrO_2 that have higher dielectric constants (*k*) than SiO_2. Recent investigations have shown that the deposition of high *k* oxides directly onto silicon can result in the formation of an SiO_2 layer that dominates the capacitance of the gate stack.[2−6] Incorporation of nitrogen in the near-surface region of silicon alleviates this problem by inhibiting SiO_2 formation during the deposition of Ta_2O_5, thereby enabling the benefits of the high *k* oxide film to be more fully realized.[7−9] Another important application of silicon nitride is as a protective coating on ceramic components such as bearings and turbine blades for which tolerance to high temperature, oxidizing environments is critical. Despite these important applications, however, the oxidation of silicon nitride films is not well understood at the molecular level. In this Article, we discuss results of an ultrahigh vacuum (UHV) investigation of the oxidation of a silicon nitride film by both gaseous atomic and molecular oxygen in which we focused our efforts on elucidating the fundamental origin for the oxidation resistance of nitrided silicon.

Several early studies have characterized the oxidation of thick silicon nitride films under conditions of high oxidant pressure.[10−13] For example, Kuiper et al. investigated the oxidation of a thick silicon nitride film by exposure to O_2 and H_2O in an atmospheric furnace. They report that the rate of oxidation of the nitride film is 2 orders of magnitude lower than the oxidation rate of Si(100) and that the presence of hydrogen (H_2 and H_2O) was necessary to oxidize the surface under the conditions examined. They assert that hydrogen reacts with the nitride to form gaseous ammonia and elemental silicon and that the surface activity toward oxidation is enhanced as a result because elemental silicon is more easily oxidized than the nitride. Similar results have been reported in studies of the dry oxidation of silicon nitride films.[11−13] While these investigations have characterized the oxidation resistance of silicon nitride at high pressure, experiments conducted under more well-defined and controllable conditions are needed to determine the underlying cause for the oxidation resistance of silicon nitride films. Experiments of this type have been reported recently by Wallace et al.[14] In this work, the investigators thermally decomposed ammonia on Si(111) to generate silicon nitride films in UHV and then

* Corresponding author. E-mail: weaver@che.ufl.edu.

10.1021/jp044434i CCC: $30.25
Published on Web 04/02/2005

oxidized the nitrided surface with molecular oxygen without breaking vacuum. From in situ analysis of the surface using X-ray photoelectron spectroscopy (XPS), the authors observed negligible oxygen uptake at surface temperatures below 873 K, and only a small amount of uptake above 873 K. The slow oxygen uptake was suggested to arise from a decrease in the concentration of surface dangling bonds after nitridation, although this effect was not quantified.

Prior investigations of the nitridation of Si(100) by NH_3 provide important insights for understanding how nitridation alters the properties of the Si(100) surface. At room temperature, ammonia adsorbs dissociatively on Si(100)-(2 × 1) to produce an adsorbed hydrogen atom and an NH_2 moiety.[15−18] Heating the ammonia-saturated surface to about 700 K then leads to the decomposition of adsorbed NH_2 and the complete desorption of hydrogen. Early investigations of this system also showed that the nitrogen atoms occupy subsurface sites after the NH_2 groups decompose.[16,19] For example, Dresser et al.[16] observed significant attenuation of the N(KLL) AES peak after sample heating, but only observed small amounts of NH_3 desorption (<10%). From these observations, Dresser et al. concluded that nitrogen migrates to the subsurface region after the adsorbed NH_2 species thermally decompose on Si(100). Subsequent studies have confirmed that nitrogen migrates to the subsurface of Si(100) during nitridation at elevated temperature (>600 K).[20−24] For example, using high-resolution photoemission, Peden et al.[21] obtained compelling evidence that silicon nitridation by NH_3 occurs by a mechanism in which nitrogen atoms diffuse into the subsurface region and leave a thin layer of elemental silicon adjacent to the vacuum−solid interface that persists as the underlying nitride film thickens. Experiments using low energy electron diffraction (LEED) also reveal that annealing the ammonia-covered surface results in a decrease in the intensity of the fractional order diffraction spots, signifying that NH_2 decomposition and nitrogen penetration to the subsurface disrupts the long-range order of the surface.[25,26] Considering that nitrogen resides below the vacuum−solid interface, direct interactions between an oxidant species and nitrogen may be expected to have only a minor influence on the oxidation behavior of nitrided Si(100). A change in the structure of the surface, as indicated by LEED experiments, may therefore be the predominant cause for the change in the reactivity of the surface toward oxidation.

Although few UHV investigations of the oxidation of silicon nitride films have been reported, the oxidation of single-crystal silicon surfaces has been studied extensively. Of particular relevance to the present work are detailed UHV studies by Engstrom et al.[27] on the oxidation of Si(100) and Si(111) by both gaseous atomic and molecular oxygen. These and other results may also be found in a review of Si oxidation written by Engel.[28] Briefly, under UHV conditions, the dissociative adsorption of O_2 on Si(100) results in an effective saturation coverage of only about 1 ML of oxygen atoms when the surface is held at 300 K during oxidation. The saturation coverage can be increased by oxidizing at elevated surface temperature, but the oxygen uptake is still rather limited. For example, the saturation oxygen coverage increases to 2 ML when Si(100) is exposed to O_2 at a surface temperature of 800 K. Not surprisingly, Engstrom et al.[27] found that gaseous oxygen atoms adsorb on Si(100) with much higher probability than does O_2 and that oxygen coverages greater than 10 ML can be obtained by oxidizing Si(100) held at 300 K using an atomic oxygen beam. In contrast to the results obtained using O_2, the uptake of oxygen atoms was found to be insensitive to the surface temperature for oxygen coverages up to about 5 ML, which is indicative of nonactivated adsorption and possibly direct insertion of gaseous O-atoms into surface Si−Si bonds.

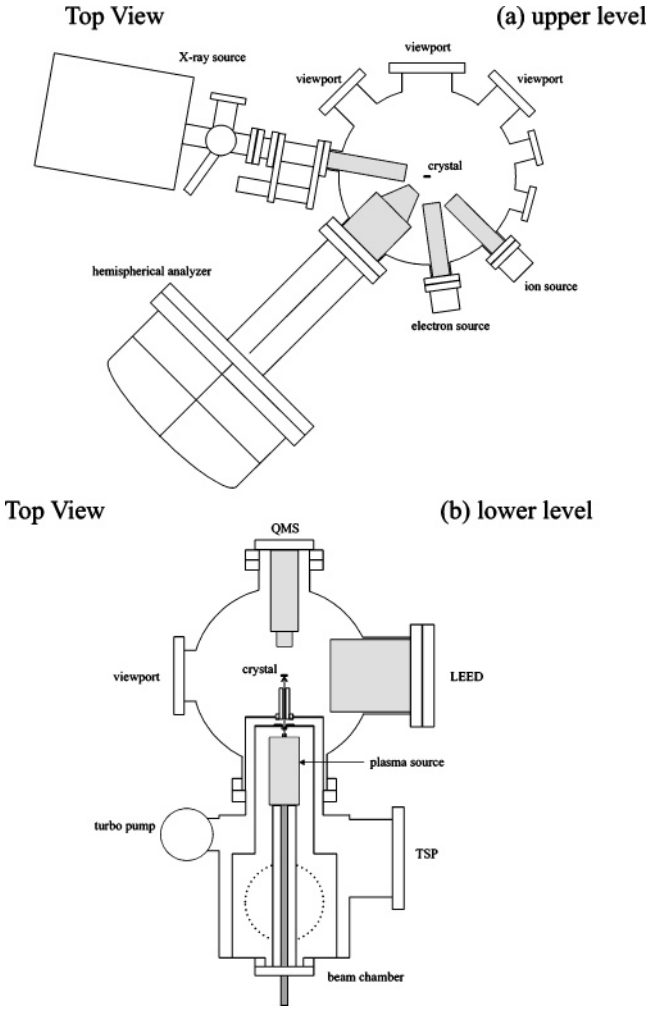

Figure 1. Top view of the (a) upper and (b) lower level of the UHV system used in the present study.

In the present study, we used X-ray photoelectron spectroscopy (XPS) to investigate the nitridation of Si(100) by the thermal decomposition of ammonia as well as the oxidation of the resulting nitride film by both gaseous atomic and molecular oxygen. The key objectives of this study were to determine the surface properties responsible for the oxidation resistance of silicon nitride films and to characterize the mechanisms for oxidation with these oxidants and the properties of oxidized nitride films. We find that surface dangling bonds play a critical role in the adsorption of both O-atoms and O_2 and provide quantitative evidence that a decrease in the surface dangling bond concentration is the primary cause for the decrease in oxygen uptake by Si(100) after nitridation.

Experimental Section

The experiments were conducted in a three-level UHV chamber that reaches a base pressure less than 2×10^{-10} Torr (Figure 1). The chamber is evacuated by an ion pump (400 L/s), a turbomolecular pump (210 L/s), and a titanium sublimation pump that is inserted into a liquid nitrogen cooled cryoshield. The upper level of the chamber (Figure 1a) houses a hemispherical analyzer (Specs EA10 plus), a dual Al/Mg anode X-ray source (Specs XR-50), a variable-energy electron source (Specs EQ 22/35), and an ion sputter source (Specs IQE 11), which

provides capabilities for performing X-ray photoelectron spectroscopy (XPS), Auger electron spectroscopy (AES), electron energy loss spectroscopy (ELS), and low energy ion scattering spectroscopy (LEISS) as well as surface cleaning by ion sputtering. The middle level of the chamber is designed primarily for gas-dosing and contains a directed doser connected to a leak valve as well as a calibrated molecular beam doser, the design of which closely follows that described by Yates.[29] The molecular beam doser is connected to a ~250 mL gas reservoir that is isolated from the UHV chamber by a pinhole gasket (10 μm aperture) and is capped by a glass microcapillary array. The pressure in the gas reservoir is measured using a capacitance monometer and can be accurately varied from 0.1 to 10 Torr. Adjusting the gas pressure in the reservoir determines the flow rate of gas through the doser and hence the impingement rate of gas molecules onto the sample surface. The lower level of the chamber (Figure 1b) houses low energy electron diffraction (LEED) optics, a two-stage differentially pumped plasma beam source, and a quadrupole mass spectrometer (QMS).

A custom-designed sample manipulator (McAllister Technical Services) is mounted to the top of the UHV chamber. Sample motion in all three Cartesian directions and sample rotation by 360° about the vertical axis is accomplished using an XY translator, a single axis translator, and a rotary platform. The specimen holder mounts to a copper reservoir that is brazed to the bottom of a stainless steel tube. The top end of the tube mounts onto the rotary platform via a flange with multiple feedthroughs for attaching thermocouples and power wires to the sample. A flat copper plate protrudes from the bottom of the copper reservoir, and L-shaped copper legs are bolted on each side of the plate, with sapphire spacers providing electrical isolation between the reservoir and the copper legs. The copper legs are each 0.25" wide, extend 2" below the bottom of the copper plate, and are separated by a distance of 1.2" from one another. A specimen is mounted to the sample holder either by directly clipping each side of the specimen to Ta plates that are bolted to the front of the flat copper legs or by spot-welding wires to both the specimen and the Ta plates. A specimen mounted to the Ta plates is in thermal contact with the copper reservoir and can be cooled to temperatures as low as 80 K when the reservoir is filled with liquid nitrogen. Samples are heated resistively and sample temperature is controlled using a PID controller to vary the output of a programmable DC supply that delivers power to the sample for heating.

The Si(100) sample used in this study was taken from an arsenic-doped (0.005 Ω cm) silicon wafer that was cut and polished to within ±0.5° of the (100) plane. An approximately 2 × 1 cm rectangular section was cut from the wafer and tightly fastened to the Ta plates that contact the cooling reservoir of the manipulator. Only tantalum parts were used to fasten the Si sample to the holder because the use of stainless steel parts was found to introduce small amounts of nickel into the sample. To measure the sample temperature, a K type thermocouple was spot-welded to a thin strip of Ta foil that was bent into a U-shape and clipped to the back of the Si(100) sample. The sample was cleaned by sputtering with 2 keV Ar^+ ions followed by annealing for several minutes at 1000 K. The sample was considered to be clean when no contaminants could be detected with XPS, and a sharp (2 × 1) LEED pattern was observed.

A two-stage differentially pumped chamber containing a commercial plasma source (Oxford Scientific Instruments) was attached to the UHV chamber (Figure 1b) and was used to generate beams containing oxygen atoms so that the initial reactivity of gas-phase oxygen atoms toward nitrided Si(100) could be investigated in the present study. Gaseous oxygen atoms are produced in this system by dissociating O_2 in a plasma that is confined to a small reservoir at the end of the plasma source. The plasma source operates at a microwave frequency (2.45 GHz) and employs electron cyclotron resonance to increase the plasma density. The plasma reservoir is fabricated from high-purity alumina to minimize atom recombination and is terminated by a 2 mm thick alumina plate that has five through holes, each of 0.4 mm diameter, that are arranged in a centered-(2 × 2) pattern within a 2 mm area. Species exit the plasma volume through these holes and form a beam that is directed toward the sample surface held in the UHV chamber. In the first pumping stage, the beam passes between oppositely charged parallel plates (±10 kV/cm) that deflect ions and electrons from the beam. After flowing through a conical skimmer ($\phi = 3$ mm) separating the first and second pumping stages, the species travel down a quartz tube before entering the UHV chamber. The quartz tube is 60 mm long and has an inner diameter of 6 mm. The quartz tube provides a lower conductance between the source and UHV chambers than would be obtained with a thin-walled orifice of the same diameter. The quartz tube also provides sufficient collimation to confine the beam to the sample surface, which facilitates reactive scattering measurements using mass spectrometry. In addition, collisions at the inner walls of the tube are expected to reduce the fraction of atoms and molecules in vibrationally and electronically excited states, which should result in beams containing primarily ground-state species, specifically $O(^3P)$ and $O_2(^3\Sigma_g^-)$. The first pumping stage of the beam chamber is evacuated with a 1200 L/s diffusion pump (Varian VHS 4), and the second stage is evacuated with a 70 L/s turbomolecular pump and a titanium sublimation pump mounted inside a liquid-nitrogen cooled cryoshield. A mechanical shutter is located in the first pumping stage to enable control over beam introduction into the main UHV chamber.

Ammonia was dosed onto the sample as a beam generated with the calibrated doser. Typical NH_3 fluxes used in these experiments were $\sim 5 \times 10^{13}$ cm^{-2} s^{-1}, which is estimated from the known NH_3 flow rate from the doser and the angular emission characteristics of microcapillary arrays.[29] Exposures of NH_3 are reported in units of ML, where 1 ML is defined as the surface atom density of 6.8×10^{14} cm^{-2} of the Si(100)-(2 × 1) surface. Pure O_2 beams were dosed onto the sample by flowing oxygen through the plasma source with the microwave power disabled. The size of the beam spot on the sample was about 9 mm in diameter. We typically employed an O_2 beam flux of 0.26 ML/s, which was determined using the spot size estimate and by comparing the O_2 pressure rise in the UHV chamber due to the beam with that resulting from a known flow rate of O_2 admitted through the calibrated beam doser. Beams containing oxygen atoms were generated by activating the microwave plasma with O_2 flowing through the source. With an initial O_2 flux of 0.26 ML/s, a measurable change in the 16 amu intensity was not observed by line-of-sight mass spectrometry when the plasma was activated. To estimate the O-atom flux, the oxygen uptake was measured on clean Si(100)-(2 × 1) held at 300 K as a function of exposure to oxygen beams with and without the microwave power enabled. From a comparison with a previous investigation of the adsorption of gaseous O and O_2 on Si(100),[27] we estimate that O-atom fluxes of ~0.001 ML/s impinged on the sample surface for the beam conditions employed. This flux is lower than expected based on the typical cracking efficiency of O_2 in the plasma source under similar operating conditions.[30]

After the oxidation experiments reported here, it was determined that the beam source was slightly misaligned with the collimating apertures, which caused substantial O-atom recombination prior to the beam entering the UHV chamber. After improving the alignment of the beam source, we performed direct mass spectrometric detection of the beam and observed an increase in the 16 amu signal when the plasma power was activated. From an analysis of mass spectrometric data, we estimate that beams with about 6% O-atoms could be routinely generated after the beam source was better aligned. We also performed threshold-ionization mass spectrometric analysis to distinguish O^+ ions generated by the direct ionization of O-atoms in the beam from those produced by the dissociative ionization of O_2. Upon enabling the plasma power, the 16 amu signal was observed to increase by more than an order of magnitude at electron energies between the direct and dissociative ionization thresholds, which is clear evidence that O-atoms are present in the plasma-activated beams. Although we employed relatively low O-atom fluxes in the experiments that are presented below, significant enhancements in the rate of oxidation were observed when the surfaces under study were oxidized at a given fluence by a plasma-activated beam versus a pure O_2 beam. This observation is consistent with previous reports of the reactivity of gaseous O as compared to O_2 toward clean Si(100)[27] and therefore provides additional evidence that gaseous O atoms and O_2 are the primary constituents of the plasma-activated beams employed in this study.

All XPS spectra reported in this study were obtained using Al Kα X-rays ($h\nu = 1486.6$ eV) with the analyzer operating in a retarding mode at a pass energy of 27 eV. The electron takeoff angle was varied by rotating the sample with respect to the analyzer axis. An angular resolution of $\pm 3°$ is estimated from the geometry of the analyzer, and electron takeoff angles are specified with respect to the surface normal. Unless stated otherwise, the spectra presented here were obtained by measuring photoelectrons emitted at an angle of 60° from the surface normal. Even at this glancing takeoff angle, the area of the sample from which photoelectrons were collected was smaller than the spot size of the oxygen beam, thus ensuring that the XPS measurements probed only the regions of the surface that were dosed with gases. The XPS spectra presented here were each processed using 21-point Savitzky−Golay smoothing, followed by background subtraction using the Shirley method.[31] Oxygen coverages were determined from the ratio of O1s to Si2p integrated intensities, and assuming that exposure of clean Si(100)-(2 × 1) at 300 K to O_2 produces a saturation coverage of 1 ML.[27,28] For the low oxygen coverages investigated here, we found it unnecessary to account for O1s and Si2p signal attenuation due to inelastic photoelectron scattering because the oxygen atoms remain in the outer surface layers. Nitrogen coverages were computed by a similar procedure, but inelastic scattering corrections were necessary in this case, as described below.

Results

NH_3 Decomposition on Si(100). An ultrathin nitride film was grown on the Si(100) substrate prior to each oxygen exposure by thermally decomposing 160 ML of ammonia on the surface at 900 K. Several layers of nitrogen incorporate into the solid during this exposure because ammonia decomposition and hydrogen desorption are rapid at 900 K.[16,22] The Si2p and N1s spectra obtained from the Si surface after this treatment are shown in Figures 2 and 3. The Si2p spectrum exhibits a main component at 99.2 eV due to elemental Si, and a smaller

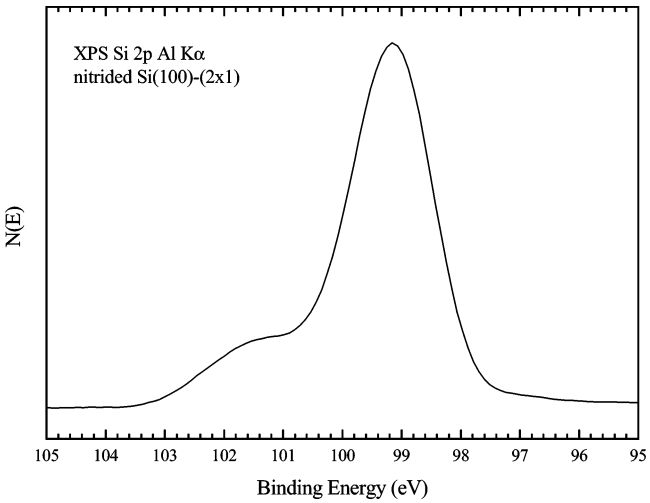

Figure 2. Si2p spectrum obtained from a Si(100) surface after a 160 ML NH_3 exposure at a surface temperature of 900 K.

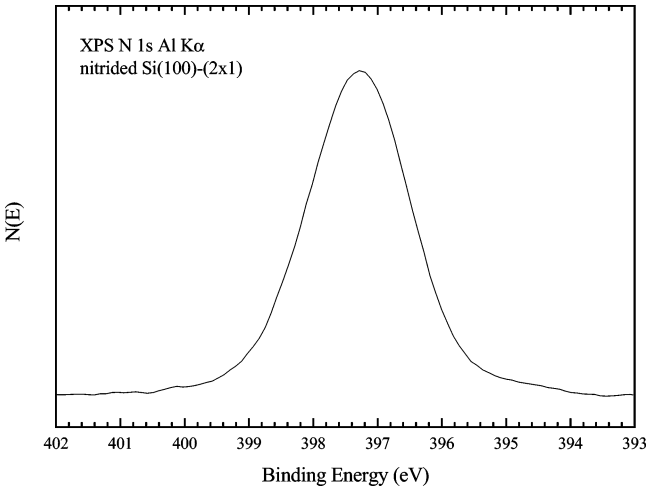

Figure 3. N1s spectrum obtained from a Si(100) surface after a 160 ML NH_3 exposure at a surface temperature of 900 K.

feature centered at about 101.8 eV. The small Si2p feature appears at a binding energy that is less than that of Si_3N_4,[21,22,24,32−35] which suggests the presence of a substoichiometric nitride. For films prepared under similar conditions, previous investigations indicate that silicon is present in a $Si_3{\equiv}N$ configuration in which each N atom is bonded with three silicon atoms. The N1s spectrum obtained after nitridation exhibits a single peak centered at a binding energy of 397.4 eV, which is also consistent with previous reports.[22,24,35,36]

Experiments were conducted to probe the interaction of NH_3 with the Si(100)-(2 × 1) surface so that the properties of the nitride film could be characterized in more detail. XPS spectra were first obtained after exposing clean Si(100) held at 300 K to a saturation dose of 160 ML of ammonia. This exposure produces a nominal coverage of 0.5 ML of adsorbed NH_2 groups, with the balance of the surface sites occupied by hydrogen atoms, and these species do not undergo further reaction at 300 K under UHV conditions.[16,20] The N1s spectrum obtained after the 300 K exposure exhibits a single peak centered at a binding energy of 398.1 eV (Figure 4a), which is consistent with previous reports of the N1s binding energy of adsorbed NH_2 on Si(100).[19] The N1s spectrum shown in Figure 4b was then obtained after annealing the amino-covered surface for 5 min at 900 K, which results in the complete desorption of hydrogen from the surface. It is noted that the spectrum did

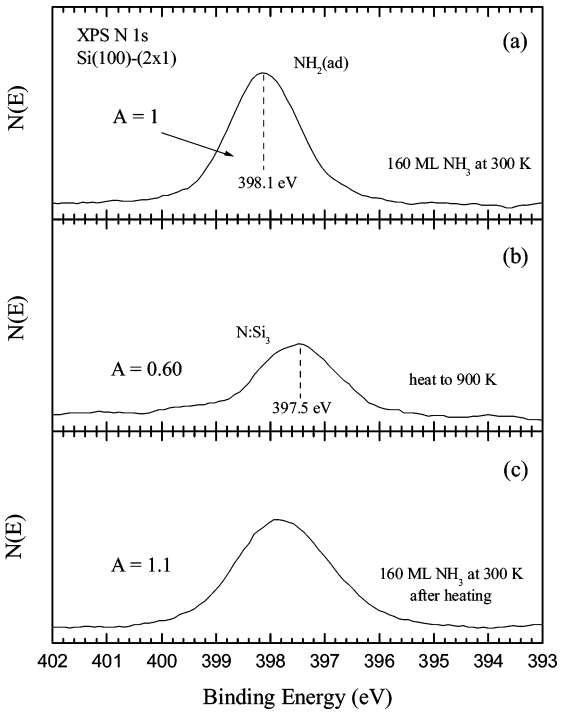

Figure 4. N1s spectra obtained from Si(100) (a) after a 160 ML NH_3 exposure at 300 K, (b) a subsequent anneal to 900 K for 5 min, and (c) a 160 ML NH_3 exposure at a surface temperature of 300 K to the surface generated in (b). The integrated areas relative to the N1s spectrum shown in (a) are indicated in each panel.

not change from that shown in Figure 4b when the sample was annealed for longer times. After annealing, the N1s peak position is shifted to a binding energy of 397.5 eV, which is consistent with the formation of $Si_3{\equiv}N$ species in the near-surface region. Annealing the amino-saturated surface also causes the N1s to Si2p intensity ratio to decrease to about 60% of its initial value. The magnitude of this decrease is in excellent agreement with that observed by Dresser et al.[16] after heating amino-saturated Si(100) to temperatures greater than about 700 K and examining the surface with AES. Dresser et al. estimated that less than 10% of the nitrogen desorbs from the surface during heating and therefore attributed the reduction in the N KLL peak intensity to nitrogen penetration into the subsurface.[16]

From the intensity changes in the N1s and Si2p spectra, we estimated the distance at which the nitrogen atoms reside below the surface after annealing the amino layer. For this calculation, nitrogen desorption is neglected, and it is assumed that all of the nitrogen atoms initially present in the amino layer reside in a single layer below the surface after the sample is heated to 900 K. It is further assumed that the probability of generating an N1s photoelectron is the same for an adsorbed NH_2 group as for the nitride. Under these assumptions, the attenuated N1s to Si2p intensity ratio of 60% can be approximated by $\ln(-x/\lambda \cos\theta)$, where x is the distance of the nitrogen atoms beneath the surface, λ is the inelastic mean free path of an N1s photoelectron through elemental Si, and θ is the photoelectron takeoff angle measured from the surface normal. Assuming an inelastic mean free path of 22.3 Å,[37] the 40% decrease in N1s peak intensity suggests that the nitrogen atoms diffuse 5.8 Å below the Si surface layer. Based on the spacing between the Si layers closest to the (100)-(2 × 1) surface, this calculation suggests that nitrogen atoms reside between the fourth and fifth layers after the amino-covered surface is annealed at 900 K. Considering the simplicity of the analysis, our estimate is in good agreement with recent electronic structure calculations, which predict that a nitrogen atom has a energetic preference to be located between the third and fourth layers of Si(100)-(2 × 1) and to bond with three Si atoms in the third layer.[23]

After annealing the initial amino layer, the surface was held at 300 K and again exposed to 160 ML of ammonia. As may be seen in Figure 4c, this exposure causes the N1s peak to grow in intensity and to shift toward higher binding energy, which indicates the presence of adsorbed NH_2 groups. Similar observations have been made by Avouris, Bozso, and Hamers[19] and indicate that annealing the amino layer partially restores the reactivity of the surface toward ammonia dissociation. According to quantum chemical calculations,[38,39] the dissociation of ammonia on Si(100)-(2 × 1) involves the adsorption of NH_3 on a single atom of a surface dimer, followed by N−H bond cleavage and hydrogen transfer to the opposing silicon atom of the dimer. Considering this prediction, it may be concluded that nitrogen diffusion into the subsurface of Si(100) regenerates pairs of surface dangling bonds, and thereby partially reactivates the surface toward ammonia dissociation. Interestingly, however, the increase in the N1s to Si2p intensity ratio after saturating the annealed surface with amino groups is only 54% of that obtained after saturating clean Si(100) with amino groups (Figure 4a). This difference suggests that nitrogen incorporation into the subsurface of Si(100) is accompanied by a structural rearrangement of the surface that reduces the density of dangling bond pairs by nearly a factor of 2 from its value on the clean surface. Indeed, in a prior study, LEED images taken after ammonia decomposition on Si(100) show a diffuse background that eclipses the fractional order spots,[25,26] indicating that nitrogen incorporation does alter the structure of the surface. The total dangling bond coverage on the nitrided surface may be estimated as 0.59 ML when all of the surface dangling bonds are assumed to exist in pairs, and taking into account attenuation of the N1s signal from subsurface nitrogen due to inelastic electron scattering from the NH_2 adsorbed at the surface.

As stated above, the procedure we employed for growing a nitride film for subsequent oxidation studies was to expose the clean surface held at 900 K to 160 ML of ammonia. The intensity of the N1s peak obtained after this procedure (Figure 3) is about 3 times greater than that obtained from the amino-saturated Si(100) surface. To estimate the thickness of the nitride film, we assume that a layered structure is formed and that each layer contains 0.5 ML of nitrogen atoms. Furthermore, based on our analysis of the amino-saturated surface before and after annealing, it is assumed that the nitride layer closest to the vacuum−solid interface resides four to five layers below the surface; this assumption is supported by the oxidation results discussed below. With these assumptions, and invoking a multilayer model to account for signal attenuation due to inelastic electron scattering, we estimate that a nitride film of 5−6 atomic layers in thickness is generated by the 160 ML ammonia exposure at 900 K. We emphasize that this film thickness is only an estimate because the analysis assumes that the nitrided region is composed of distinct layers, each with 0.5 ML of nitrogen atoms, and hence that the nitride−Si interfaces (upper and lower) are atomically abrupt. While the interfaces are unlikely to be perfectly abrupt, the oxidation results suggest that nitrogen atoms reside in only small concentrations in the topmost three layers. The findings from these experiments that have a key impact on the understanding of oxidation of the nitrided surface are (1) that the nitride films produced by ammonia decomposition on Si(100) reside in the subsurface region and (2) that nitridation reduces the density of surface dangling bond sites.

Oxidation of Nitrided Si(100) at 300 K. *Atomic versus Molecular Oxygen.* Oxidation of the nitrided surface by both molecular and atomic oxygen was investigated at a surface temperature of 300 K. After nitridation, the surface was exposed to the oxygen beam for 60 min, and the surface was then analyzed with XPS. A 60 min beam exposure corresponds to ~930 ML of O_2 for the fluxes employed. Exposing the nitrided surface to the pure O_2 beam for 60 min results in an oxygen coverage of 0.27 ML, which was found to be the limiting coverage for oxidation of the nitrided surface at 300 K by O_2. The oxygen coverage increased to 1.2 ML when the nitrided surface was exposed to the same beam fluence but with the plasma power enabled. This result shows that gas-phase oxygen atoms are significantly more reactive toward nitrided Si(100) than is O_2, particularly considering that only about 3 ML of oxygen atoms are estimated to have impinged on the surface during the 60 min exposure. The much higher reactivity of atomic oxygen is not surprising considering that the initial adsorption probabilities of gaseous O and O_2 on clean Si(100)-(2 × 1) are reported to be 1 and 0.03, respectively.[27] The O1s feature obtained after oxidizing with the plasma-activated beam is very similar in shape and peak location to that obtained after oxidizing with O_2 at 300 K (not shown). The O1s peak is shifted to a higher binding energy by 0.1 eV after oxidizing with the plasma-activated beam, as compared to oxidation with pure O_2, but this shift is consistent with the higher oxygen coverage that is achieved with the atomic oxygen beam. It is well known that as the coverage of oxygen is increased, the oxygen atoms on the Si(100) surface experience changes in their bonding environment that alters the O1s binding energy.[27,28] The similarities in the O1s spectra indicate that gaseous oxygen atoms and molecules produce similar chemical states of oxygen on the nitrided surface, which suggests that after adsorption (or O_2 dissociation) the processes by which oxygen atoms incorporate into the nitrided surface are independent of the identity of the gaseous oxidant. It therefore follows that the enhanced uptake achieved with the plasma-activated beam is due to the higher adsorption probability of oxygen atoms as compared to O_2 on the nitrided surface.

Clean versus Nitrided Si(100). A comparison of the oxygen uptake on the clean and nitrided Si(100) surfaces reveals that nitridation significantly lowers the surface reactivity toward oxidation. For example, exposing the clean surface to 930 ML of O_2 at 300 K results in an oxygen coverage of about 1 ML, whereas a coverage of only 0.27 ML is reached on the nitrided surface by oxidizing under the same conditions. The difference in the reactivity of these surfaces toward gaseous oxygen atoms is less pronounced, but is still quite significant. Specifically, an oxygen coverage of 1.2 ML is obtained by exposing the nitrided surface at 300 K to the plasma-activated beam for 60 min, whereas a coverage of 2.1 ML is obtained on the clean surface for the same exposure and surface temperature. Because the nitride film is shown to reside several layers below the vacuum−solid interface, the lower reactivity of the nitrided surface as compared to the clean surface does not arise from a direct interaction between nitrogen and oxygen (vide infra) but is attributed to the lower concentration of dangling bonds on the nitrided surface.

Chemical State Changes Induced by Oxidation at 300 K. Shown in Figures 5−7 are the Si2p, N1s, and O1s spectra obtained from the nitrided surface after depositing 1.2 ML of atomic oxygen at a surface temperature of 300 K. Also shown are the Si2p and N1s spectra obtained from the nitrided surface before oxidation, and the O1s spectrum obtained after exposing clean Si(100)-(2 × 1) held at 300 K to a saturation dose of O_2, which results in about 1 ML of atomic oxygen on the surface. Each spectrum has been normalized by its peak height to facilitate comparison. Among all of these spectra, the most distinct change caused by oxidation is an increase in the intensity of a feature centered at about 102 eV in the Si2p spectrum (Figure 5). This spectral change indicates an increase in the amount of Si atoms present in partially oxidized states as oxygen atoms are incorporated within the nitrided surface. As discussed below, this feature is assigned specifically to Si^{2+} and Si^{3+} species that are directly bonded to oxygen atoms in the outermost surface layers.

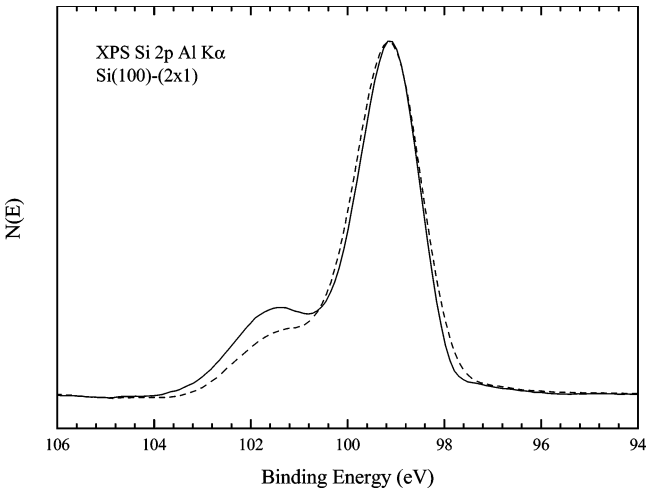

Figure 5. Si2p spectra obtained after exposing clean Si(100) to 160 ML NH_3 at a surface temperature of 900 K (− − −), and after depositing 1.2 ML of oxygen on the nitrided Si(100) surface held at 300 K using the plasma-activated beam (−).

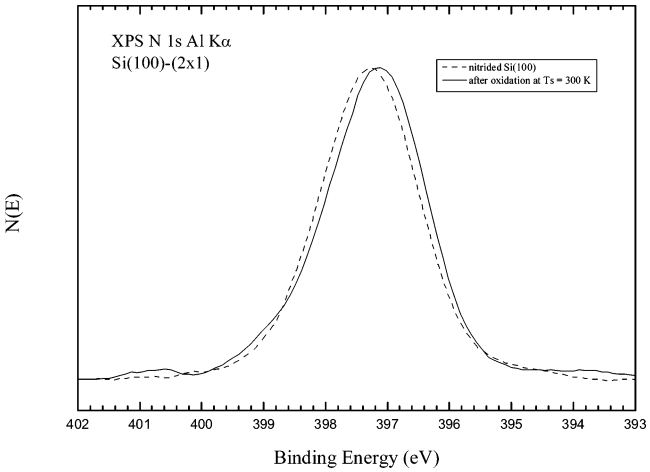

Figure 6. N1s spectra obtained after exposing Si(100) to 160 ML NH_3 at a surface temperature of 900 K (− − −), and after depositing 1.2 ML of oxygen on the nitrided Si(100) surface held at 300 K using the plasma-activated beam (−).

The N1s spectra obtained before and after oxidation at 300 K are shown in Figure 6. Oxidation causes small changes in the N1s feature, but the changes observed are reproducible and distinct. In particular, after oxidation the center of the N1s peak is shifted to lower binding energy by about 0.2 eV, and a small feature appears at a binding energy of 399.2 eV. Previous studies have reported that Si_2═N−O structures give rise to an N1s feature at a binding energy of about 399 eV.[40,41] The appearance of the high binding energy shoulder is therefore consistent with a small quantity of N−O bonds being formed upon oxidation at 300 K. This observation suggests that only a small fraction

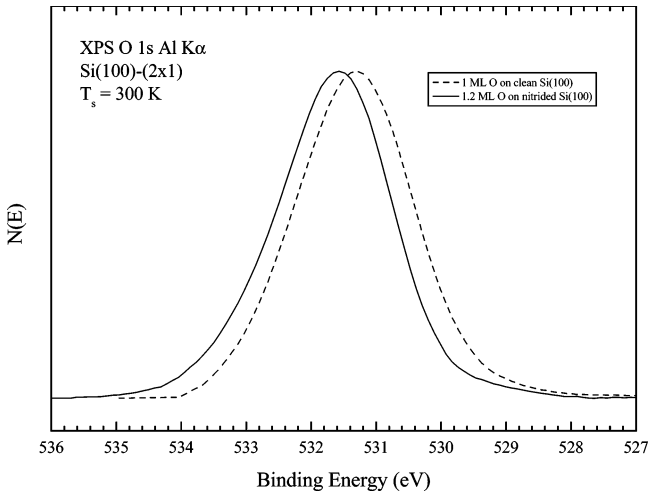

Figure 7. O1s spectra obtained after incorporating 1 ML of oxygen atoms on Si(100) at a surface temperature of 300 K (− − −), and after depositing 1.2 ML of oxygen on the nitrided Si(100) surface held at 300 K using the plasma-activated beam (−).

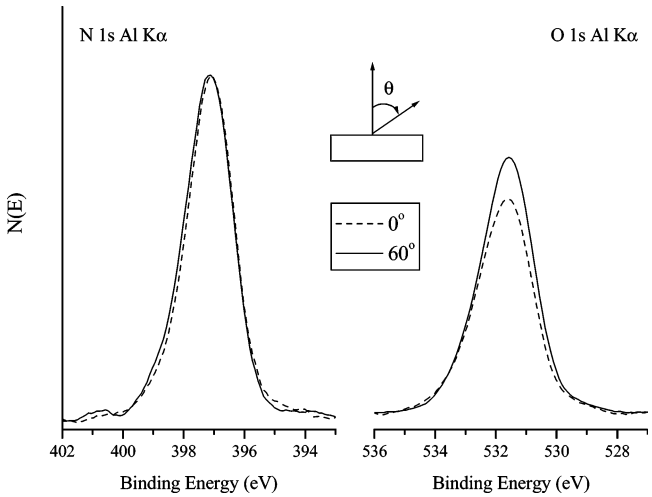

Figure 8. N1s and O1s spectra obtained at electron collection angles of 0° (− − −) and 60° (−) after depositing 1.2 ML of oxygen on nitrided Si(100) at a surface temperature of 300 K. The O1s and N1s peak heights have been normalized to the N1s peak height at the respective angle.

of oxygen atoms diffuse to the subsurface Si−nitride interface and bond with nitrogen. In addition, nitrogen atoms may be present in very small concentrations in the topmost three layers, so Si_2═N−O structures may exist in these layers as well. In either case, the small amount of N−O bonding that is detected suggests that the nitride−Si interface is rather sharp.

The incorporation of both nitrogen and oxygen atoms in the near-surface region of Si(100) has been found in most cases to cause the N1s peak to shift to a higher binding energy (BE) relative to the N1s BE obtained from pure nitride surfaces.[23,40,41] A positive binding energy shift of the N1s peak may result from a core-hole screening effect that arises from the formation of a dielectric film near the vacuum−solid interface. However, such a screening effect should be negligible for the films we have investigated because no more than 2 ML of oxygen atoms are present at the outer surface. Positive BE shifts of the N1s feature have also been attributed to a second nearest neighbor (NN) interaction in which oxygen atoms withdraw charge from Si atoms that are directly bonded to nitrogen in the film.[23,40] The negative binding energy shift of the main N1s feature observed in the present study suggests that at 300 K the majority of oxygen atoms do not penetrate far enough below the vacuum−solid interface to occupy second NN positions with respect to the nitrogen atoms. The small shift of the N1s peak to lower binding energy could be caused by the introduction of strain at the nitride−Si interface when oxygen atoms are incorporated into the top surface layers. Because these spectra show that the majority of the N and O atoms in the film do not directly interact, the growth of the 102 eV feature in the Si2p spectrum following oxidation may be attributed to the formation of Si^{2+} and Si^{3+} species that are directly bonded to oxygen atoms in the outermost surface layers.

The O1s spectra obtained after depositing 1 and 1.2 ML of oxygen on the clean and nitrided surfaces, respectively, at 300 K are shown in Figure 7. The O1s peak obtained from the nitrided surface after oxidation is similar in shape to that obtained from the pure oxide layer, but is shifted to higher binding energy by about 0.3 eV. This difference in binding energies indicates that oxygen atoms at a concentration of about 1 ML experience slightly different chemical environments when adsorbed on clean versus nitrided Si(100) at 300 K. Based on the small N1s feature observed at 399 eV, a small fraction of the oxygen atoms appear to be directly bonded with nitrogen atoms in the film. This bonding interaction could alter the O1s binding energy and produce a shift from the binding energy obtained from the pure oxide film. In addition, the oxygen atoms near the vacuum−solid interface, which do not directly bond with nitrogen, may experience a different chemical environment than a similar quantity of oxygen atoms incorporated into the clean surface. Such an effect could arise if the structures in the near-surface layers of the solid differ for the clean and nitrided surfaces. This latter interpretation is consistent with the ammonia uptake experiments, which show that nitridation lowers the surface dangling bond density, probably by inducing a structural change at the surface.

Angle-Resolved XPS Data. The chemical changes suggested by the XPS spectra provide the general picture that oxidation of the nitrided surface at 300 K results in nearly segregated oxide and nitride layers, with the oxide layer being closer to the vacuum−solid interface. To further examine this possibility, XPS spectra were obtained at different photoelectron takeoff angles to vary the depth resolution of the measurements. Shown in Figure 8 are the O1s and N1s spectra collected at 0° and 60° takeoff angles with respect to the surface normal after adsorbing 1.2 ML of oxygen atoms on the nitrided surface at 300 K. To illustrate the variation in the O1s/N1s intensity ratio with average sampling depth, the spectra obtained at a given takeoff angle are scaled by the integrated intensity of the N1s spectrum measured at that angle. Qualitative differences in the spectra obtained at different collection angles are slight, suggesting that the chemical states of nitrogen and oxygen remain fairly uniform throughout the film. The slight broadening of the N1s feature toward high binding energy at glancing takeoff angle may arise from a small amount of N−O bonding at the nitride−oxide interface closest to the surface. The most distinct difference between these spectra is clearly the increase of approximately 15% in the O1s/N1s intensity ratio for the measurements performed at a 60° takeoff angle, that is, the more surface sensitive configuration. This result confirms that the oxygen atoms reside closer to the outer surface of the solid than do the nitrogen atoms when as much as 1.2 ML of oxygen atoms are adsorbed on nitrided Si(100) at 300 K.

Oxidation of Nitrided Si(100) at 800 K. *Atomic versus Molecular Oxygen.* Oxidation of the nitrided surface by both atomic and molecular oxygen was also investigated at a surface

TABLE 1: Oxygen Coverages on Clean and Nitrided Si(100)

	atomic oxygen[b]		molecular oxygen[b]	
	300 K	800 K	300 K	800 K
[O] (nitrided)[a]	1.2	1.5	0.27	0.85
[O] (clean)[a]	2.1	2.4	1.0	2.0
nitrided/clean	0.57	0.62	0.27	0.44

[a] Oxygen coverages [O] are given in units of ML, as defined in the text, and were obtained after exposing the surface to the oxidant beam for 60 min at the surface temperatures indicated. [b] The columns labeled "atomic" and "molecular" oxygen correspond, respectively, to beam exposures with and without the plasma power enabled.

temperature of 800 K for comparison with the oxidation behavior observed at 300 K, and to therefore assess the influence of surface temperature on oxidation. Increasing the surface temperature from 300 to 800 K significantly enhances the reactivity of the nitrided surface toward O_2. In particular, exposing the nitrided surface to 930 ML of pure O_2 produces an atomic oxygen coverage of 0.85 ML when the surface is held at 800 K, which appears to be a saturation coverage for these oxidation conditions. In contrast, only 0.27 ML of oxygen is deposited by exposing the nitrided surface to O_2 at 300 K. The enhancement in reactivity with increasing surface temperature is less pronounced when oxidizing with oxygen atoms. For example, exposing the nitrided surface to the plasma-activated beam for 60 min produces oxygen coverages of 1.2 and 1.5 ML when the surface is held at 300 and 800 K, respectively. This is only a 25% increase in oxygen uptake, which is much lower than the 215% increase that is brought about by increasing the surface temperature when O_2 is used as the oxidant. Despite the small enhancement in oxygen uptake with surface temperature, a higher oxygen coverage is still obtained by oxidizing with gaseous O-atoms at 800 K as compared to O_2.

Similarities in the O1s spectra (not shown) indicate that similar chemical states of oxygen are generated on the nitrided surface when oxidation is conducted using either gaseous oxygen atoms or molecules at a surface temperature of 800 K. Thus, after adsorption (or O_2 dissociation), the processes by which oxygen atoms incorporate into the solid again appear to be independent of the identity of the gaseous oxidant, at least for the low coverages considered. The O1s peak does shift to higher binding energy by about 0.2 eV as the oxygen coverage on the nitrided surface is increased from 0.85 to 1.5 ML. However, this is a small difference in binding energy, considering that the oxygen coverage is nearly doubled, so it may be concluded that the increase in oxygen coverage from 0.85 to 1.5 ML causes only minor alterations to the chemical bonding environment of oxygen atoms incorporated into the nitrided surface at 800 K.

Clean versus Nitrided Si(100). Table 1 summarizes the oxygen coverages obtained by oxidizing the nitrided and clean surfaces at the conditions indicated. Examination of the coverages given in the table shows that the influence of surface temperature on oxygen uptake is similar for the nitrided and clean Si(100) surfaces. For example, a 930 ML O_2 exposure to clean Si(100)-(2 × 1) generates oxygen coverages of 1.0 and 2.0 ML at surface temperatures of 300 and 800 K, respectively. These coverages are in good agreement with previous studies[27,28] and demonstrate that oxygen uptake by the clean surface is enhanced considerably by increasing the surface temperature when O_2 is used as the oxidant, which is similar to the behavior found for the nitrided surface. As was also observed for the nitrided surface, increasing the surface temperature produces a smaller increase in oxygen uptake by the clean surface when oxidizing with gaseous oxygen atoms. Table 1 shows that

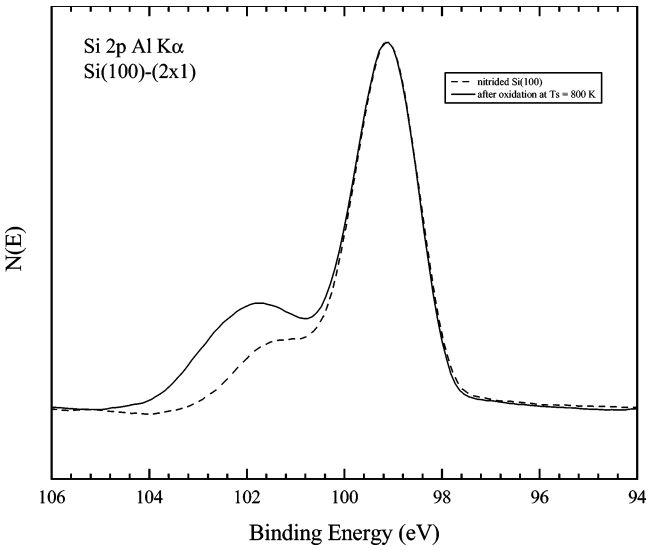

Figure 9. Si2p spectra obtained after exposing clean Si(100) to 160 ML NH_3 at a surface temperature of 900 K (− − −), and after depositing 1.5 ML of oxygen on the nitrided Si(100) surface held at 800 K using the plasma-activated beam (−).

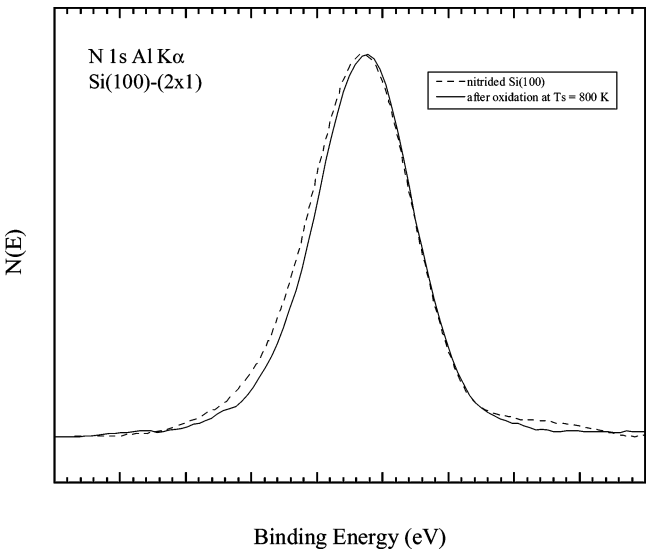

Figure 10. N1s spectra obtained after exposing Si(100) to 160 ML NH_3 at a surface temperature of 900 K (− − −), and after depositing 1.5 ML of oxygen on the nitrided Si(100) surface held at 800 K using the plasma-activated beam (−).

oxygen coverages of 2.1 and 2.4 ML result after exposing the clean surface to the plasma-activated beam for 60 min with the surface temperature maintained at 300 and 800 K, respectively. In the work by Engstrom et al.,[27] it was found that atomic oxygen adsorption on the clean Si(100) surface remains independent of the surface temperature up to oxygen coverages of 4−5 ML. Thus, the relative insensitivity to surface temperature that we observed when oxidizing with the plasma-activated beam is expected for the oxygen coverages examined (<3 ML). We do observe a small enhancement in uptake from the plasma-activated beam with increasing surface temperature. However, because O_2 is by far the majority beam component, this small enhancement in uptake most likely reflects the influence of surface temperature on O_2 incorporation.

Chemical State Changes Induced by Oxidation at 800 K. Figures 9−11 display the Si2p, N1s, and O1s spectra obtained after oxidizing the nitrided surface with oxygen atoms at a surface temperature of 800 K, which produces an oxygen

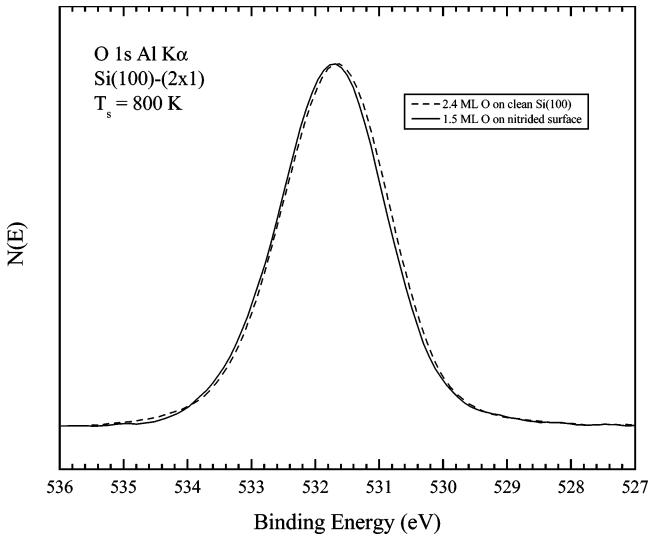

Figure 11. O1s spectra obtained after incorporating 2.4 ML of oxygen atoms on Si(100) at a surface temperature of 800 K (− − −), and after depositing 1.5 ML of oxygen on the nitrided Si(100) surface held at 800 K using the plasma-activated beam (−).

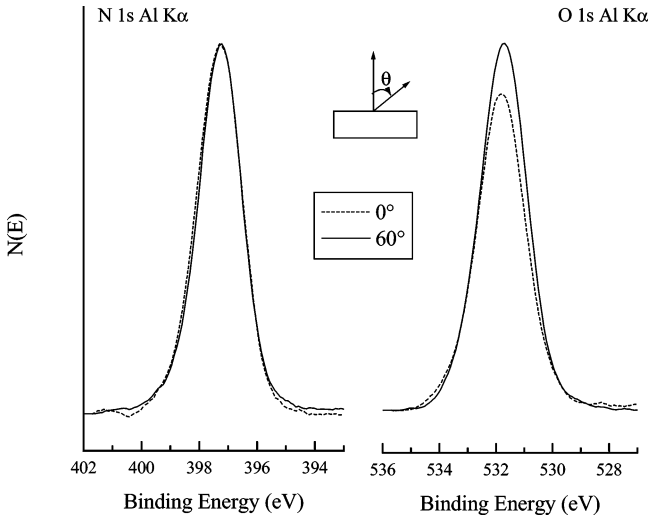

Figure 12. N1s and O1s spectra obtained at electron collection angles of 0° (- - - -) and 60° (−) after depositing 1.5 ML of oxygen on nitrided Si(100) at a surface temperature of 800 K. The O1s and N1s peak heights have been normalized to the N1s peak height at the respective angle.

coverage of 1.5 ML. Figures 9 and 10 also show the Si2p and N1s spectra obtained from the nitrided surface before oxidation, and Figure 11 shows an O1s spectrum after depositing 2.4 ML of oxygen onto the clean Si(100) surface. Each spectrum has been normalized to its respective peak height to augment the contrasting features. The most pronounced spectral change following oxidation at 800 K is an increase in the intensity of the high binding energy feature in the Si2p spectrum (Figure 9) that is centered at about 102 eV and extends to 104 eV. The appearance of this feature indicates that Si^{+n} ($n > 0$) states are generated during oxidation of the nitrided surface. While similar results were obtained following oxidation at 300 K (Figure 5), the intensity of the high BE Si2p feature is clearly greater and the feature extends to higher BE when oxidation is conducted at 800 versus 300 K. The formation of a higher concentration of Si^{+n} species not only arises from the higher oxygen coverages that are obtained during high temperature oxidation, but also from temperature-dependent changes in the oxidation process. For example, for nearly the same oxygen coverage, we find that oxidation at 800 versus 300 K results in a greater amount of Si^{2+}, Si^{3+}, and Si^{4+} states. This observation is consistent with the oxidation behavior of clean Si(100)-(2 × 1).[28] At 300 K, oxidation occurs more uniformly across the surface, with the average Si oxidation state increasing in proportion to the oxygen coverage. Increasing the surface temperature enhances surface atom mobility and results in the formation of more highly oxidized clusters at relatively low oxygen coverage. The incorporation of oxygen into oxidized areas of the surface likely alleviates strain in the surface layers during oxidation.

Shown in Figure 10 are the N1s spectra obtained before and after oxidizing the nitrided surface at 800 K to reach an oxygen coverage of 1.5 ML. After oxidation, the N1s peak is slightly narrower and the peak maximum is shifted by only about 0.1 eV to lower binding energy. Because these spectral changes are slight, it may be concluded that the nitrogen bonding environment is altered negligibly during oxidation at 800 K, at least when the oxygen coverage is increased up to 1.5 ML. Furthermore, the BE shift is in the direction opposite to that observed when O and N atoms occupy second NN sites,[23,40,41] which suggests that the oxygen and nitrogen atoms in the film remain segregated, even though oxidation at elevated temperature enhances surface atom mobility, as evidenced by the formation of Si^{3+} and Si^{4+} oxidation states at low oxygen coverage (Figure 9). Interestingly, the N1s BE shift is smaller than that observed after oxidation at 300 K (compare Figure 10 to Figure 6), and the small feature at 399.2 eV is not evident in the N1s spectrum. These observations suggest that segregation of the nitride and oxide phases occurs to a greater extent at elevated surface temperature, with immeasurable formation of $Si_2{=}N{-}O$ structures. Because the growth of highly oxidized SiO_x clusters involves substantial surface restructuring, it is conceivable that oxidation at elevated temperature enables the subsurface nitride to adopt a more favorable structure in which nitrogen atoms experience a more uniform bonding environment. Such a change may explain the slight narrowing of the N1s peak observed after oxidation of the nitrided surface at 800 K.

The O1s spectra obtained after oxidizing the clean and nitrided Si(100) surfaces at 800 K to oxygen coverages of 2.4 and 1.5 ML are remarkably similar (Figure 11). The slightly lower BE of the O1s peak maximum obtained from the pure oxide probably arises from the higher oxygen concentration on that surface. Indeed, the similarity between the O1s spectra indicates that the presence of a nitride in the subsurface of Si(100) has a negligible influence on the chemical state(s) of oxygen that form during oxidation at 800 K. Thus, it appears that SiO_x regions with similar properties grow on clean and nitrided Si(100) during oxidation at 800 K, despite the structural differences of these surfaces. The similarity in the O1s spectra (Figure 11) is also consistent with enhanced segregation of the oxide and nitride phases when oxidation is conducted at elevated surface temperature.

Angle-Resolved XPS Data. Analysis of the XPS spectra obtained after oxidizing the nitrided surface at 800 K provides evidence that the oxidized and nitrided regions remain segregated. Angle-resolved XPS spectra provide additional support for this interpretation. Figure 12 shows the O1s and N1s spectra obtained at electron takeoff angles of 0° and 60° with respect to the surface normal, after adsorbing 1.5 ML of oxygen on the nitrided surface at 800 K. To compare the O1s/N1s intensity ratio as a function of sampling depth, the spectra obtained at a given angle have been normalized with respect to the N1s intensity at that angle. Only minor qualitative changes in the spectra obtained at different takeoff angles are observed. For example, the O1s peak obtained at a 60° takeoff angle is shifted

by only 0.1 eV to lower binding energy relative to the O1s peak obtained at an emission angle of 0°. Differences between the N1s spectra obtained at these takeoff angles are slight. Similar to the angle-resolved data obtained after oxidizing at 300 K, the O1s/N1s ratio increases by about 10% when the collection angle is adjusted to the more surface sensitive configuration. This observation confirms that oxygen resides closer to the vacuum−solid interface than does the nitride region.

Discussion

The present results show that nitridation of Si(100) at elevated temperature reduces the concentration of surface dangling bonds by nearly a factor of 2 and that the reactivity of the surface toward both atomic and molecular oxygen decreases significantly. Because the XPS results also reveal that the majority of oxygen and nitrogen atoms do not directly interact within the films studied, but remain in nearly segregated layers, the decrease in surface dangling bond concentration appears to be the primary cause for the diminished activity of the nitrided surface. Physically, this conclusion implies that both gaseous oxygen atoms and molecules adsorb predominantly, if not exclusively, at dangling bond sites or pairs on the surface and that the uptake of oxygen by the nitrided surface is limited by the availability of such sites. That dangling bonds are the active sites for O_2 adsorption is not at all surprising. In fact, quantum chemical calculations predict that the lowest energy pathway for O_2 activation on Si(100)-(2 × 1) involves the formation of a peroxy species across a surface dimer.[42]

It is perhaps more surprising that gaseous oxygen atoms have such a strong tendency to adsorb at dangling bond sites because this implies that insertion directly into Si−Si bonds occurs to a negligible extent. While it is possible that an O atom incident from the gas phase must overcome an activation barrier to directly insert into a Si−Si bond, we consider this possibility to be unlikely because formation of a Si−O−Si linkage is exothermic by at least 6 eV. A propensity for oxygen atoms to adsorb at dangling bonds, rather than to directly insert into Si−Si bonds, may be explained if we assume that the majority of oxygen atoms in the beam exist in the ground ^3P electronic state and then consider electron spin effects. Because the ^3P state is a triplet, direct O-atom insertion into a Si−Si bond is strictly spin-forbidden, whereas adsorption at a dangling bond site is not. In this case, the rate at which O-atoms from the beam directly insert into Si−Si bonds would be limited by the rate of nonadiabatic curve crossing events that transform the electronic configuration of the incident oxygen atom to a state such as the singlet ^1D state for which direct insertion is allowed. Such events are likely to be rare in a single gas−surface collision at thermal impact energy. Thus, the observation of selective O-atom adsorption at surface dangling bond sites suggests that the initial adsorption event tends to be electronically adiabatic for the beam conditions employed.

A quantitative comparison of the uptake of oxygen by the clean and nitrided Si(100) surfaces provides additional insight for understanding the role of dangling bonds in the oxidation of these surfaces. The bottom row of Table 1 shows the oxygen coverages obtained on the nitrided surface relative to that obtained on the clean surface for various oxidizing conditions. As may be seen in the table, the oxygen coverages obtained by exposing the nitrided surface to the atomic oxygen beam at surface temperatures of 300 and 800 K are 57% and 62.5% lower than that obtained on the clean surface. These values are remarkably close to the ratio of dangling bond concentrations on the nitrided and clean surfaces (59%) and provide quantitative evidence that gaseous O-atoms adsorb preferentially on surface dangling bonds on both surfaces. This comparison is even more favorable when considering that the contribution of O_2 to the uptake achieved during the plasma-activated beam exposure is more significant at a surface temperature of 800 K. Interestingly, for oxidation with O_2, the maximum oxygen coverage obtained on the nitrided surface at 300 K is only 27% of that obtained on the clean surface (Table 1). This value is less than one-half of the ratio of dangling bond concentrations on the nitrded versus clean surfaces. Assuming that an O_2 molecule does dissociate across a single dimer on the clean Si(100)-(2 × 1) surface, as predicted by electronic structure calculations,[42] this comparison suggests that at least two dimers are consumed when a single oxygen molecule dissociates and the oxygen atoms incorporate into the nitrided surface at 300 K. While it is difficult to envision four dangling bonds being required to activate one O_2 molecule, it is conceivable that dangling bond pairs could be arranged on the nitrided surface in such a way that O_2 activation on one pair could render a neighboring pair unable to readily activate a second O_2 molecule. The uptake of oxygen on the nitrided surface increases to 44% of that on the clean surface when oxidation is conducted at 800 K using O_2, which may indicate that fewer dangling bond pairs are consumed or are more efficiently regenerated on the nitrided as compared to the clean surface during oxidation at elevated temperature. Overall, these observations suggest that oxidation with gaseous oxygen atoms occurs by a similar mechanism on the clean and nitrided surfaces, with the main difference being that fewer adsorption sites are available on the nitrided surface. In contrast, the mechanism for O_2 dissociative chemisorption and oxygen incorporation appears to be more sensitive to structural differences between the nitrided and clean surfaces.

Increasing the surface temperature enhances the uptake of O_2 on both the clean and the nitrided surfaces, but produces only a small increase in the uptake of gaseous O-atoms. High surface temperatures are thought to facilitate the oxidation of clean Si(100) by O_2 by promoting oxygen penetration into the subsurface layers.[28] Such penetration is likely to regenerate dangling bond sites at the surface that are needed to activate O_2 molecules, thereby restoring the surface activity toward O_2 dissociation. It is noted that a molecular beam study by Ferguson et al.[43] shows that the dissociation probability of O_2 on Si(100) is only weakly dependent on the surface temperature at low gas temperatures. Thus, more facile regeneration of active surface sites is the more likely explanation for the enhancement in oxygen uptake with surface temperature than would be promotion of O_2 bond cleavage at higher surface temperature.

A relative insensitivity to surface temperature in the uptake of gaseous O-atoms by Si(100) was first observed by Engstrom et al.[27] and was quite reasonably interpreted by those authors as evidence that oxygen atoms incident from the gas-phase insert readily into Si−Si bonds. The uptake of gaseous O-atoms, believed to be predominantly O(^3P), was found to increase with surface temperature only at oxygen coverages greater than about 4−5 ML, which corresponds to oxygen atoms inserted into all of the Si−Si bonds that are directly accessible from the gas phase. However, the findings from the current study indicate that surface dangling bonds are the preferred adsorption site for a gaseous O-atom and that direct insertion into a Si−Si bond is relatively unimportant. Considering this finding, it is difficult to understand why an increase in the surface temperature effects only a small enhancement in the uptake of gaseous oxygen atoms. In particular, if more effective regeneration of surface dangling bond sites is the primary reason that an increase in

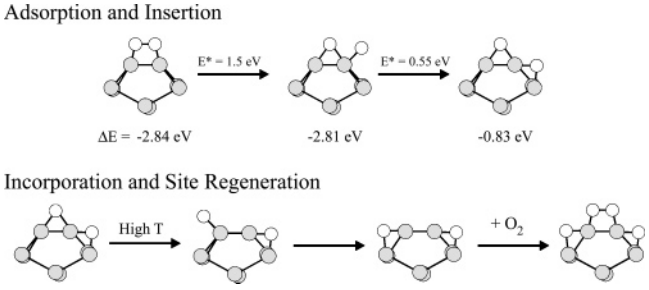

Figure 13. Model for O_2 dissociation and incorporation into Si(100). The top panel shows the structures and energetics for the dissociative chemisorption of O_2 on Si(100) as predicted by DFT calculations.[42] The bottom panel shows possible elementary steps for oxygen migration to the subsurface that results in the regeneration of an empty dimer. White circles represent oxygen atoms, and gray circles represent silicon atoms.

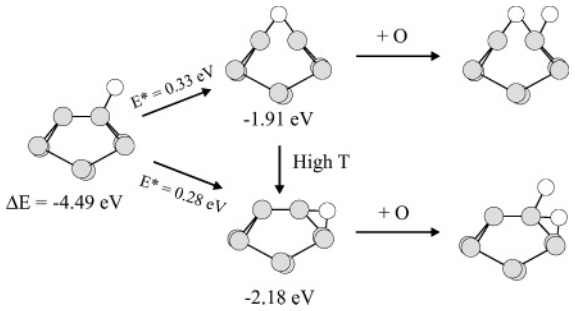

Figure 14. Model for O-atom adsorption and incorporation into Si(100). The energy changes, where indicated, were predicted using DFT calculations as reported in ref 42. White circles represent oxygen atoms, and gray circles represent silicon atoms.

surface temperature enhances O_2 uptake, then it is reasonable to expect that the uptake of gaseous oxygen atoms would also be promoted by raising the surface temperature because O-atoms also adsorb selectively at dangling bond sites and more of these sites should be available at high surface temperature.

A recent computational investigation by Widjaja and Musgrave[42] may offer a plausible explanation for understanding the different effects of surface temperature in the oxidation of Si(100) with gaseous O atoms versus O_2. The top panel of Figure 13 shows a schematic of key structures and the associated energy changes that were predicted to occur by those authors when O_2 adsorbs and then dissociates on the Si(100)-(2 × 1) surface.[42] It is important to note that the molecular representations shown in Figures 13 and 14 are only intended to depict the steps in the proposed model and do not precisely illustrate the bond lengths and angles for these structures as predicted by density functional theory. Following adsorption, the O_2 molecule is predicted to span the dimer to form a peroxy-like species that then dissociates to produce an oxygen atom inserted across the dimer and a siloxy radical. The oxygen atom of the siloxy radical then inserts into a Si−Si back-bond, resulting in the final structure shown in the top panel. Clearly, the formation of a second peroxy species on the final structure would be significantly hindered by the presence of the O-atom bridging the dimer. Thus, if the oxygen atoms in this final structure have limited mobility, then effectively only one O_2 molecule can dissociate for each dangling bond pair on the surface. Notice that this situation would result in an oxygen coverage of 1.0 ML on the Si(100)-(2 × 1) surface and may help to explain the substantial reduction in oxygen uptake that occurs at 1.0 ML when the clean surface is exposed to O_2 at 300 K.

The bottom panel of Figure 13 illustrates elementary steps by which the bridging oxygen atom could migrate to a back-bond site. These reactions have not been explored computationally as far as we know. The first step in the scheme shows the formation of a siloxy radical by cleavage of an Si−O bond of the bridging oxygen species, and the second step involves oxygen insertion into a Si−Si back-bond. This migration process regenerates an empty dimer and would thereby enable a second O_2 molecule to bind in the peroxy configuration. Although energy barriers for these steps have not been explicitly predicted, the results of Widjaja and Musgrave suggest that the first step, production of the siloxy radical, should have the larger energy barrier. This barrier may be comparable to the 1.38 eV barrier required for the reverse of the final reaction step shown in the top panel of Figure 13. Considering the large energy barrier, the migration of the bridging oxygen atom to a back-bond site should be promoted significantly by raising the surface temperature. Thus, according to this mechanism, oxygen uptake by O_2 dissociation is enhanced at elevated surface temperature because the population of empty dimers increases with increasing surface temperature.

Shown in Figure 14 are pathways proposed for the incorporation of a gaseous oxygen atom into the Si(100) surface. Based on the present results, the O-atom is assumed to adsorb initially on a dangling bond site to form a siloxy radical. From this site, the oxygen atom can insert either across the surface dimer or into a Si−Si back-bond to form the structures shown in the figure. The energy changes illustrated in this figure were also taken from the work of Widjaja and Musgrave and show relatively small differences in the energetics of these insertion pathways. Because an O-atom adsorbs at a single dangling bond site, and therefore does not have the strict steric requirements for adsorption as does O_2, we speculate that a second O-atom will adsorb with roughly equal probability on each of the one O-atom structures shown in Figure 14. Thus, according to this interpretation, an increase in surface temperature has only a minor influence on the uptake of gaseous oxygen atoms because enhanced oxygen migration to subsurface sites does not significantly affect the availability of single dangling bond sites at the surface.

Conclusions

We have investigated the nitridation of Si(100) and the subsequent oxidation of this surface by both gaseous atomic and molecular oxygen under UHV conditions. Nitridation of Si(100) by the thermal decomposition of ammonia at 900 K results in the formation of a subsurface nitride and a decrease in the concentration of surface dangling bond sites. On the basis of changes in N1s spectra after NH_3 adsorption and decomposition, we estimate that the nitride resides four to five layers below the vacuum−solid interface and that the concentration of dangling bonds on the nitrided surface is about 0.59 ML or 59% of that on the clean surface. Oxidation of the nitrided surface at surface temperatures of 300 and 800 K produces an oxide phase that resides in the outer surface layers and remains largely segregated from the subsurface nitride for oxygen coverages up to about 2.5 ML. At a surface temperature of 300 K, the incorporation of about 1 ML of oxygen into the near surface layers alters the nitrogen bonding environment only slightly, most likely by introducing strain in the subsurface nitride, and the N1s spectra indicate that a small quantity of Si_2═N−O also forms. At 800 K, the nitride bonding environment changes negligibly for oxygen coverages as high as 2.5 ML, which is consistent with greater segregation of the nitride and oxide phases and enhanced structural relaxation in these phases. In addition, at a given oxygen coverage, the quantity of Si^{3+} and

Si^{4+} states that are detected increases when oxidation is conducted with the surface held at 800 versus 300 K, indicating a tendency for regions of high local oxygen concentration to form at elevated temperature.

The reactivity of Si(100) toward both atomic and molecular oxygen decreases significantly after nitridation of the subsurface region due to the decrease in surface dangling bond concentration that accompanies nitride growth. Quantitative support for this conclusion is given by the observation that, for the same exposure to gaseous oxygen atoms, the oxygen coverage obtained on the nitrided surface relative to that on clean Si(100) is within 5% of the ratio of dangling bond concentrations on these surfaces. This finding also provides evidence that gaseous $O(^3P)$ atoms adsorb initially at dangling bond sites on these surfaces and that direct insertion into Si−Si bonds occurs to a negligible extent. An increase in surface temperature is found to significantly enhance oxygen uptake by the nitrided surface when O_2 is used as the oxidant, but brings about only a slight increase in uptake when gaseous oxygen atoms are employed. It is proposed that an increase in surface temperature promotes oxygen migration to the subsurface, and thereby results in more effective regeneration of empty dimers. Because the activation of an O_2 molecule on the Si(100) surface has more stringent steric requirements than does O-atom adsorption, the facile penetration of oxygen to the subsurface at high temperature has a greater influence on the adsorption of O_2 than O.

Acknowledgment. We thank Paulo Herrera for technical assistance with the initial experiments performed in this study. We also gratefully acknowledge funding for this work provided by the National Science Foundation through grant number NSF-CTS 0207291.

References and Notes

(1) Takahashi, M.; Tamura, M.; Asuha; Kobayashi, T.; Kobayashi, H. *J. Appl. Phys.* **2003**, *90*, 726.

(2) Park, S. W.; Baek, Y. K.; Lee, J. Y.; Park, C. O.; Im, H. B. *J. Electron. Mater*. **1992**, *21*, 635.

(3) Hitchens, W. R.; Krusell, W. C.; Dobkin, D. M. *J. Electrochem. Soc.* **1993**, *140*, 2615.

(4) Wilk, G. D.; Wallace, R. M.; Anthony, J. M. *J. Appl. Phys.* **2001**, *89*, 5243.

(5) Devine, R. A. B. *Appl. Phys. Lett.* **1996**, *68*, 1924.

(6) Atanassova, E.; Spassov, D. *Appl. Surf. Sci.* **1998**, *135*, 71.

(7) Luan, H. F.; Wu, B. Z.; Kang, L. G.; Kim, B. Y.; Vrtis, I. R.; Roberts, I. D.; Kwong, D. L. *IEDM Tech. Dig.* **1998**, 373.

(8) Park, D.; Lu, Q.; King, T. J.; Hu, C.; Kalnitsky, A.; Tay, S. P.; Cheng, C. C. *Proc. IEDM Tech. Dig.* **1998**, 381.

(9) Passacantando, M.; Jolly, F.; Lozzi, L.; Salerni, V.; Picozzi, P.; Santucci, S.; Corsi, C.; Zintu, D. *J. Non-Cryst. Solids* **2003**, *322*, 225.

(10) Kuiper, A. E. T.; Willemsen, M. F. C.; Mulder, J. M. L.; Elferink, J. M. L.; Habraken, F. H. P. M.; Vanderweg, W. F. *J. Vac. Sci. Technol., B* **1989**, *7*, 455.

(11) Raider, S. I.; Flitsch, R.; Aboaf, J. A.; Pliskin, W. A. *J. Electrochem. Soc.* **1976**, *123*, 560.

(12) Murarka, S. P.; Chang, C. C.; Adams, A. C. *J. Electrochem. Soc.* **1979**, *126*, 886.

(13) Hayafuji, Y.; Kajiwara, K. *J. Electrochem. Soc.* **1982**, *129*, 2102.

(14) Wallace, R. M.; Wei, Y. *J. Vac. Sci. Technol., B* **1999**, *17*, 970.

(15) Taylor, P. A.; Wallace, R. M.; Choyke, W. J.; Dresser, M. J.; Yates, J. T. *Surf. Sci*. **1989**, *215*, L286.

(16) Dresser, M. J.; Taylor, P. A.; Wallace, R. M.; Choyke, W. J.; Yates, J. T. *Surf. Sci*. **1989**, *218*, 75.

(17) Larsson, C. U. S.; Flodström, A. S. *Surf. Sci.* **1991**, *241*, 353.

(18) Zhou, X.-L.; Flores, C. R.; White, J. M. *Surf. Sci. Lett.* **1992**, *268*, L267.

(19) Avouris, Ph.; Bozso, F.; Hamers, R. J. *J. Vac. Sci. Technol., B* **1987**, 1387.

(20) Larsson, C. U. S.; Andersson, C. B. M.; Prince, N. P.; Flodström, A. S. *Surf. Sci.* **1992**, *271*, 349.

(21) Peden, C. H. F.; Rogers, J. W., Jr.; Shinn, N. D.; Kidd, K. B.; Tsang, K. L. *Phys. Rev. B* **1993**, *47*, 15622.

(22) Ishidzuka, S.; Igari, Y.; Takaoka, T.; Kusunoki, I. *Appl. Surf. Sci.* **1998**, *132*, 107.

(23) Kim, J. W.; Yeom, H. W.; Kong, K. J.; Yu, B. D.; Ahn, D. Y.; Chung, Y. D.; Whang, C. N.; Yi, H.; Ha, Y. H.; Moon, D. W. *Phys. Rev. Lett.* **2003**, *90*, 106101-1.

(24) Kim, J. W.; Yeom, H. W. *Surf. Sci.* **2003**, *546*, L820.

(25) Glachant, A.; Saidi, D.; Delford, J. F. *Surf. Sci.* **1986**, *168*, 672.

(26) Chérif, S. M.; Lacharme, J.-P.; Sébenne, C. A. *Surf. Sci.* **1992**, *262*, 33.

(27) Engstrom, J. R.; Bonser, D. J.; Engel, T. *Surf. Sci*. **1992**, *268*, 238.

(28) Engel, T. *Surf. Sci. Rep*. **1993**, *18*, 91.

(29) Yates, J. T. *Experimental Methods of Surface Science*; AIP Press: New York, 1998 and references therein.

(30) Schmidt, A. A.; Offermann, J.; Anton, R. *Thin Solid Films* **1996**, *281*, 105.

(31) Shirley. *Phys. Rev. B* **1972**, *5*, 4709.

(32) Miyazaki; Narasaki, M.; Suyama, A.; Yamaoka, M.; Murakami, H. *Appl. Surf. Sci*. **2003**, *216*, 252.

(33) Brijs, B.; Deleu, J.; Conard, T.; De Witte, H.; Vandervorst, W.; Nakajima, K.; Kimura, K.; Genchev, I.; Bergmaier, A.; Goergens, L.; Neumaier, P.; Dollinger, G.; Dobeli, M. *Nucl. Instrum. Methods Phys. Res., Sect. B* **2000**, *161*, 429.

(34) Gritsenko, V. A.; Svitasheva, S. N.; Petrenko, I. P.; Novikov, Y. N.; Morokov, Y. N.; Wong, H.; Kwok, R. W.; Chan, R. W. M. *Microelectron. Reliab.* **1998**, *38*, 745.

(35) Seino, T.; Muto, D.; Matsuura, T.; Murota, J. *J. Vac. Sci. Technol., B* **2002**, *20*, 1431.

(36) Hlil, E. K.; Kubler, L.; Bischoff, J. L.; Bolmont, D. *Phys. Rev. B* **1987**, *35*, 5913.

(37) Kubler, L.; Bischoff, J. L.; Bolmont, D. *Phys. Rev. B* **1988**, *38*, 13113.

(38) Widjaja, Y.; Musgrave, C. B. *Phys. Rev. B* **2001**, *64*, 205303−1.

(39) Xu, X.; Kang, S.-Y.; Yamabe, T. *Phys. Rev. Lett.* **2002**, *88*, 076106-1.

(40) Bhat, M.; Yoon, G. W.; Kim, J.; Kwong, D. L.; Arendt, M.; White, J. M. *Appl. Phys. Lett*. **1994**, *64*, 2116.

(41) Kim, J. W.; Yeom, H. W.; Chung, Y. D.; Jeong, K.; Whang, C. N. *Phys. Rev. B* **2002**, *66*, 035312−1.

(42) Widjaja, Y.; Musgrave, C. B. *J. Chem. Phys.* **2002**, *116*, 5774.

(43) Ferguson, B. A.; Reeves, C. T.; Mullins, C. B. *J. Chem. Phys.* **1999**, *110*, 11574.